Perspective

High-Throughput Methods Using Composition and Structure Spread Libraries

John R. Kitchin and Andrew J. Gellman
Dept. of Chemical Engineering, Carnegie Mellon University, Pittsburgh, PA 15213

DOI 10.1002/aic.15294
Published online May 27, 2016 in Wiley Online Library (wileyonlinelibrary.com)

Introduction

Many properties of multicomponent materials of interest in chemical engineering, e.g., viscosity, catalytic activity, stability, etc…, depend on the material composition and the environment in which the material is used. The ability to predict quantitatively how these properties depend on the composition of the material and on environmental variables is essential to enabling the optimal design of materials and operating conditions, as well as prediction of material's performance under suboptimal conditions. Unfortunately, the necessary measurements of material properties vs. composition are not commonly available and the ability to calculate their properties at arbitrary compositions is extremely challenging.

Traditionally, it has been time-consuming and costly to map materials properties across composition and environmental conditions. This is a combinatorial problem, which quickly becomes intractable because there are many relevant degrees of freedom (material components, environmental components, temperature, pressure, etc…) which are enumerated by continuous variables. The conventional approach to mitigate this problem is to limit the number of components, compositions or conditions, and to perform discrete experiments to sample the relevant degrees of freedom. Nearly all progress in chemical engineering, materials science and other materials related disciplines has resulted from this approach, but there is a growing recognition that it is slow and expensive. As technologies advance, the expectations of materials properties become increasingly stringent and the types of materials that meet these expectations become increasingly complex and difficult to design. It takes 10–20 years to translate a new material from discovery into commercial applications. The recently announced Materials Genome Initiative (MGI)[1] is a large effort funded by the US government to stimulate the acceleration of new materials from discovery to commercialization at twice the traditional speed and at a fraction of the cost. There are several approaches to the MGI, including computational,[2] experimental,[3] and hybrid approaches that use both experiments and computations.[4] These are having a significant impact on corporate R&D processes and they will impact research across the Chemical Engineering discipline.

This perspective describes the application of combinatorial libraries that are continuous composition spreads of metallic alloys, or spreads of another property such as surface structure or nanoparticle size, and is not intended to be a comprehensive review of high-throughput methods. We refer interested readers to the following published reviews in materials,[5] heterogeneous catalysis,[6,7] homogeneous catalysis,[8] and automotive applications.[9] For high-throughput computational approaches to these areas we refer to these published reviews.[10–17] The work described in this perspective differs from most of these reviews in the utilization and spatial characterization of samples with continuous or near-continuous gradients in some property, e.g., composition, structure, or particle size.

In this perspective, we describe innovations in experimentation and computations by our research groups and others that have the potential to contribute significantly to the development of multicomponent materials for engineering applications. We describe new experimental methods and instrumentation that enable the synthesis and characterization of samples with gradients in alloy composition, surface structure, nanoparticle size, etc… and their characterization across composition, structure and size space using spatially resolved analytical tools. This reduces the need to make numerous discrete samples, perform discrete experiments, and simultaneously results in richer and higher quality datasets defining structure/composition/property relationships. We will illustrate the utility of these methods with examples from studies of alloy corrosion/oxidation resistance, alloy catalysis and electrocatalysis. These examples show how properties vary across composition, surface structure, and nanoparticle size spaces, and in some cases under different environmental conditions. We will also show how computational simulation has been integrated into these studies, providing guidance on what properties to study, and confirmation of how to interpret datasets that span entire alloy composition spaces. We end with our thoughts on the opportunities and the needs of high throughput methodologies as applied in chemical engineering.

Correspondence concerning this article should be addressed to J. R. Kitchin at jkitchin@andrew.cmu.edu.

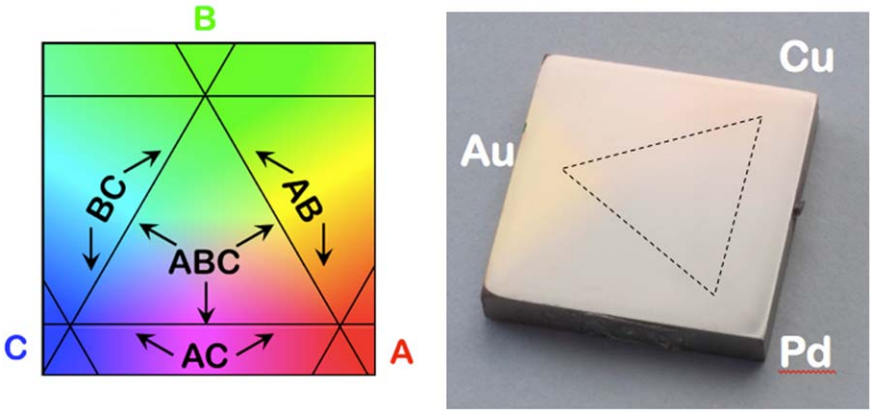

Figure 1. Left. Graphic illustration of a ternary CSAF deposited in the form of a thin film (typically <1 μm) on a substrate that can be 1–10 cm in lateral dimensions. The triangular region at the center contains all possible compositions of the ternary material $A_xB_yC_{1-x-y}$ with $x=0\rightarrow1$, $y=0\rightarrow1-x$. Along its edges are regions containing the three binary composition spreads. At the vertices are regions that contain the three single components in pure form. Right. Photograph of a $Cu_xAu_yPd_{1-x-y}$ CSAF deposited as a 100 nm thick film on a 2.5 × 14 × 14 mm³ polished Mo substrate.

Composition Alloy Spread Films

High throughput methods typically rely on the use of "libraries," physical samples that contain large numbers of different materials that can be prepared, characterized and studied simultaneously or, at least, using highly automated data collection. One of the advantages of these libraries is that all samples contained within the library can be treated identically during heating, exposure to environment, aging, etc... Similarly, parallelized measurement methods allow collection of data with higher internal self-consistency than in sets of discrete measurements. The 96-well plates commonly used in many biochemical laboratories are one example of a high throughput library. In many materials research laboratories including ours, the composition spread alloy film (CSAF) has become the common form of materials library (Figure 1).[18–21]

A typical need in the fields of catalysis, corrosion, and others, is to know how some property depends on the composition of a multicomponent metal catalyst, alloy material, etc... In catalysis, it is known that the activity of an alloy can be different than that of its components. Traditionally, the activity has been studied by making discrete catalyst samples of different compositions, with individual characterization of the samples and individual measurements of catalytic activity and selectivity. This approach has made remarkable progress over the past century, but it is time consuming, labor intensive and consequently, expensive. Since it is typical to have only a small number of samples, it can be difficult to determine trends in reactivity with great confidence, and to decouple the trends in observed activity from other effects such as particle size which may also vary with catalyst composition. Surface science studies of thin alloy films on single crystal substrates provides one approach to creation and study of a model system, but again typically one alloy composition is studied at a time, and each sample is time-consuming to synthesize, characterize and study.

An alternative approach to the study of alloy films of a single uniform composition is to make and characterize CSAFs, thin alloy films with a composition gradient across the sample (Figure 1), for use in studies of catalysis. When CSAFs are coupled with spatially resolved analysis tools one can, in essence, characterize many samples across composition space in a single experiment. The key is to create high quality, well-characterized gradients. Gellman and co-workers have designed and fabricated an ulta-high vacuum deposition chamber, the rotating shadow mask (RSM) CSAF deposition apparatus, that allows up to 4 metals to be simultaneously co-deposited on a substrate surface with controlled gradients.[22,23] The deposition flux gradients are created using the shadow mask concept.[18] By controlling the deposition rates from each metal evaporation source, and the orientations of rotatable shadow masks that control gradient orientations, an entire ternary alloy composition space (or subspace) can be made as a CSAF. For example, in a ternary alloy $A_xB_yC_{1-x-y}$ the full space of $x=0\rightarrow1, y=0\rightarrow1-x,$ and $z=0\rightarrow1-x-y$ can be made on a single surface. This alloy library includes the pure components at the corners of a triangle, the three binary alloy CSAFs along the edges of the triangle, and the ternary alloy space in the interior of the triangle. The RSM-CSAF deposition tool can also create samples with magnified subspaces spanning the library or quaternary CSAFs with the fourth component held at constant composition across the substrate.

The utility of these CSAF libraries lies in the ability to measure alloy characteristics such as the bulk composition, surface composition, bulk atomic structure, electronic structure, etc... all as continuous functions of local CSAF composition. These can then be correlated to spatially resolved measurements of functional properties such as catalytic activity, corrosion passivation, hardness, etc... In the next sections, we illustrate specific applications of CSAFs in the areas of corrosion and catalysis. The first example from a study of alloy corrosion will describe the creation of Fe-Ni-Al alloy CSAFs and a study of their oxidation resistance via formation of a protective alumina scale. The second example will illustrate the measurement of surface and catalytic properties of binary Cu-Pd CSAFs spanning composition space.

Corrosion

Materials corrosion is an issue of significant industrial concern and societal impact. Corrosion results from the oxidation

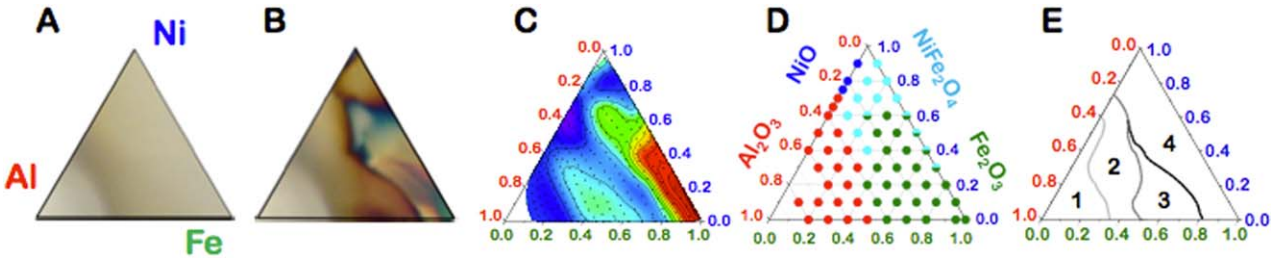

Figure 2. Oxidation of an $Al_xFe_yNi_{1-x-y}$ CSAF mapped across composition space.

(A) Photograph of the $Al_xFe_yNi_{1-x-y}$ CSAF as prepared. (B) Photograph of the $Al_xFe_yNi_{1-x-y}$ CSAF after oxidation at 700 K for 4 h in dry air. The observable discolorations are very reproducible and clearly allow visual differentiation of oxidation behaviors. (C) A map of the oxygen uptake by the alloy films as measured using energy dispersive x-ray (EDX) analysis. The Fe rich regions exhibit the highest level of oxidation (red) while the Al rich region are passivated (blue). (D) Raman mapping of the oxide phases (Al_2O_3, NiO, $NiFe_2O_4$, and Fe_2O_3) formed across compositions space. E. The four regions of $Al_xFe_yNi_{1-x-y}$ composition space exhibiting distinct oxidation behavior. The critical aluminum concentration, below which bulk oxidation occurs, is indicated by the boundary of region 4.

of a metal to an oxide or dissolved ionic form. One way to combat corrosion is to add corrosion resistant components to the metal, e.g., by alloying or coating. Doing so often compromises some other property, e.g., the mechanical strength, or cost, so finding the alloy composition that optimizes these multiple properties is essential. Given that structural alloy can have as many as 10–12 components, rigorous optimization of properties becomes infeasible by traditional means.

A typical corrosion passivation additive is a metal that will segregate to the surface of the alloy and form a protective oxide scale that is impenetrable to environmental oxidants. For example, Cr will segregate to the surface of a Ni containing alloy and form an adherent, protective chromium oxide surface layer that hinders further corrosion. Aljohani et al. used a CSAF to study the corrosion resistance of Ni-Cr films as measured by electrochemical screening.[24] The films were deposited on a 10 × 10 array of electrodes on a silicon substrate. They were able to characterize the composition and structure of the films on the electrodes, as well as perform independent electrochemical characterization of *each individual electrode*. They found that particular phases of the alloy occurring at specific compositions showed the highest resistance to corrosion, whereas in composition regions with co-existence of phases, there is less resistance to corrosion.

The study of gas phase alloy oxidation can also be accelerated using high throughput methods.[25–27] Ni/Al alloys are commonly referred to as superalloys because they maintain structural integrity at temperatures up to 80% of their melting points. Aluminum is added to provide corrosion resistance because it segregates to the alloy surface, generating a protective aluminum oxide scale. Very early work led to the concept of the critical aluminum concentration, Ni^*_{Al}, above which corrosion is passivated under operating conditions.[28] The amount of Al required has been fine-tuned over decades of experience with Ni/Al alloys. Ni, however, is relatively expensive, and it is desirable to reduce the amount of Ni present by alloying with a cheaper metal such as Fe. The downside is that Fe is more readily oxidized, and a greater fraction of Al is required to protect the ternary $Al_xFe_yNi_{1-x-y}$ alloy. Adding too much Al is detrimental to the mechanical properties of the alloy, and hence an optimal composition that minimizes cost, and that maximizes mechanical properties and oxidation resistance is desired. The addition of Fe to the alloy complicates the process of finding the critical Al concentration because it now becomes a trajectory through ternary alloy composition space, $Ni^*_{Al}(x, y)$ rather than a scalar quantity. Gellman and coworkers approached this problem by examining the oxidation behavior in dry air of a ternary $Al_xFe_yNi_{1-x-y}$ CSAF.[26]

The goal of that study of $Al_xFe_yNi_{1-x-y}$ oxidation was to identify the critical aluminum concentration required to form a protective aluminum oxide scale on the alloy and to map its path through composition space (Figure 2). EDX was used to map the uptake of oxygen across $Al_xFe_yNi_{1-x-y}$ CSAFs exposed to dry air at 700 K (Figure 2C). Subsequently, Raman spectroscopy (Figure 2D), x-ray photoelectron spectroscopy (XPS) depth profiling, and SEM imaging were used to map and characterize the oxidation behavior across composition space. The combined datasets have allowed identification of four distinct regions of oxidation behavior and the boundaries between them in composition space (Figure 2E). In region 1, a protective surface scale of Al_2O_3 clearly formed. In regions 2 and 3, the alloy is passivated by a continuous but subsurface Al_2O_3 scale with an external Fe_2O_3 scale forming over the Al_2O_3. The two regions are differentiated by whether the scale is smooth (region 2) or rough (region 3). Region 4 is not passivated and deep oxidation was observed. In summary, the boundary on the Al rich side of region 4 defines the composition dependent critical aluminum concentration required to protect the alloy from deep oxidation in dry air at 700 K. This single study of oxidation on a single CSAF library has yielded a high fidelity picture (Figure 2) of ternary alloy oxidation that would have required years of work by traditional methods!

Catalysis

Metal alloys are used frequently in catalysis because it has been found empirically that the alloys often exhibit catalytic performance superior to those of their elemental components.[29] Not surprisingly, the activity of an alloy depends on its composition, and in many cases the optimal composition depends on the reaction conditions. The conventional approach to finding this optimal composition, or to understanding the composition dependence of alloy reactivity has been to synthesize alloy samples at discrete compositions, and characterize them in detail. While nearly everything we know about alloy catalysis has been determined using this approach, it is slow and expensive, and has limited progress.

One challenge to designing alloys to have specific surface properties is that the surface composition often differs from the bulk composition due to surface segregation. Segregation in

alloys or multicomponent mixtures occurs when changes to the surface composition lower the free energy of the system, e.g., because an element with a lower surface energy segregates to the surface, or when larger atoms segregate to the surface to relieve strain in the bulk. By measuring the surface composition of a sample as a function of temperature, one can determine the segregation energy *at that bulk composition*, which can be used to estimate the surface composition at other temperatures. The segregation energy may be a function of composition itself, but performing experiments on alloys with enough different compositions to determine this function is rarely done.

Miller et al. used a Cu_xPd_{1-x} CSAF to thoroughly map the segregation behavior of a Cu-Pd alloy.[30] In that work, they used XPS and low energy ion scattering spectroscopy (LEIS) to measure the bulk and surface compositions of a Cu_xPd_{1-x} CSAF at different temperatures and different bulk compositions. They also used electron backscatter diffraction to identify the composition dependent bulk phases in the CSAF. They observed that the composition dependent phase behavior of the film closely resembled bulk phase behavior, with a B2 phase forming at intermediate compositions, as expected, and FCC solid solutions forming at Cu-rich and Pd-rich compositions.[31] The temperature dependent LEIS data revealed Cu segregation at all Cu_xPd_{1-x} compositions ($x_{Cu} = 0.05$–0.95) and temperatures (400–1000 K) but with a maximum at 700 K. The Langmuir-McLean segregation model was used to extract composition dependent enthalpies and entropies of segregation from measurements spanning composition space on *a single sample*, including robust estimates of error in the measurements.

Alloying can result in a change in the electronic structure of the metal components; this is often one reason for the changed reactivity. XPS core level shifts (CLS) are sensitive probes of the local chemical environment, e.g., the local composition, structure, ordering, and strain state, of atoms in an alloy. Boes et al. used a composition spread Cu-Pd alloy film to study how the CLS of the alloy components varied with composition.[32] Previous reports of the CLS from numerous samples of fixed compositions[33,34] indicated that the Cu CLS decreases monotonically and nearly linearly across the entire composition space. These samples had all been annealed at high temperatures, and were likely in an FCC solid solution phase. In contrast, Boes' work using a CSAF showed an anomalous dip in the Cu CLS in the range of $0.33 < x_{Pd} < 0.55$. Electron backscatter diffraction showed that in this composition range the bulk phase has a B2 structure, which is body-centered cubic analogous to the CsCl structure. Density functional theory calculations were used to show that the anomalous dip in the CLS was due to the existence of the *ordered* B2 phase, and that the anomaly disappears when the solid FCC solution forms.

In catalysis, a primary goal has been to correlate the electronic structure of the catalyst with its reactivity. The direct correlation of *experimentally* measured electronic structure and *experimentally* measured reactivity across composition space is rare. We have demonstrated above that it is possible to combine the CSAFs and high spatial resolution spectroscopies to map out electronic structure, bulk phases, surface composition, etc… across composition space. Measuring reactivity is more difficult and requires development of specialized reactor systems for high throughput measurements of catalytic activity.[35–38] Gellman's lab has developed a novel microreactor system to address this need using CSAF libraries.[39] They created a 20×10 array of channels in a solid glass block to form the inlet and outlet channels of a 10×10 array of microreactors. The CSAF and the microreactor array are compressed together, but separated by a thin gasket having a 10×10 array of 700×900 μm^2 holes that isolate 100 regions of different composition across the CSAF surface (Figure 3). Each channel is isolated, and allows gases to flow to the CSAF surface, react, and then flow through its corresponding outlet channel to a mass spectrometer for analysis. Since the channels and the holes in the gasket are arranged in space, they sample different compositions across the CSAF catalyst library, and conventional reaction kinetics experiments can be conducted, e.g., partial pressure dependence, temperature dependence, etc… at 100 different alloy compositions, in parallel.

The microreactor was used in two recent studies that examined the reactivity of a Cu_xPd_{1-x} CSAF for H_2-D_2 exchange.[40,41] In that work, the conversion of H_2 to HD was measured at 100 locations on the CSAF as a function of temperature (300–600 K). A microkinetic model that described dissociative adsorption, and recombinative desorption of H_2, D_2, and HD was used to derive an expression for the temperature dependent conversion. The model was then fitted to the experimental data to derive *composition-dependent* activation energies for adsorption and desorption. The results were in good agreement with previous studies on alloys of fixed composition. More importantly they provided estimates of $\Delta E^{\ddagger}_{ads}(x)$ and $\Delta E^{\ddagger}_{des}(x)$ across composition space (Figure 4A).

In parallel, ultraviolet photoelectron spectroscopy (UPS) was used to map the valence bands of the Cu_xPd_{1-x} alloy across composition space. The valence bands in Cu-Pd are dominated by the *d*-bands, and since they are nearly filled, UPS approximately measures the *d*-band properties of this alloy. DFT calculations showed that the trends in the *d*-band center vs. alloy composition are similar to those of the valence band (containing *s*, *p*, and *d* electrons), and that this is the same trend observed in the average energy of the valence band measured experimentally using UPS (Figure 4B). This enabled us to make one of the first experimentally determined correlations between the alloy electronic structure and reactivity across a continuous alloy composition space (Figure 4C).

The composition dependent barrier to H_2 adsorption on Cu_xPd_{1-x} alloys is not a simple linear interpolation of the barriers on Cu and Pd across the composition space. On the Pd-poor side of the composition range, the H_2 adsorption barrier decreases with an approximately linear dependence on Pd composition. The adsorption barriers were lower than a simple linear interpolation of the pure metal properties would suggest. Above $x_{Pd} = 0.40$, however, this trend ceased, with adsorption barriers becoming independent of Pd composition. To investigate this phenomenon, we developed a novel approach to modeling composition spread alloy surfaces using density functional theory.[41] We found that the region of near linear decrease in adsorption barriers with lower values than suggested by linear interpolation of the pure component values, $x_{Pd} < 0.40$ were readily explained by hydrogen-induced segregation of Pd to the surface. In other words, the surface composition was richer in Pd than it would be under vacuum conditions. Because Pd is the more active component this results in lower barriers. The change in behavior for $x_{Pd} > 0.40$ cannot be explained so simply, and may be due to the

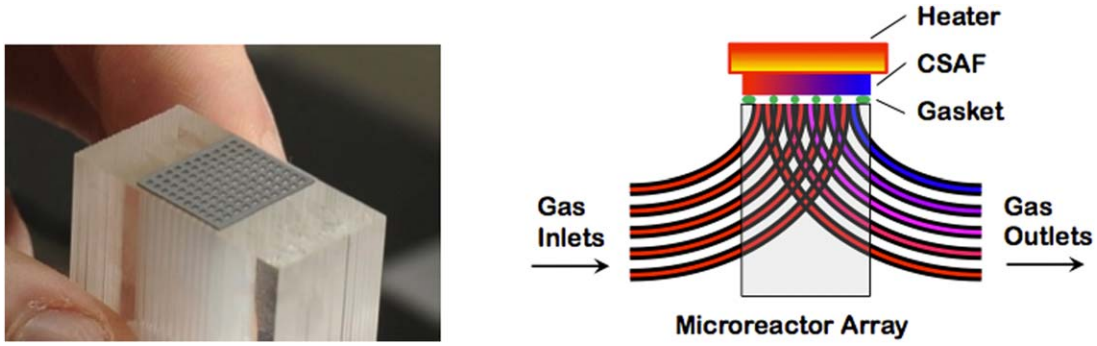

Figure 3. Left. Photograph of the glass microreactor array consisting of 100 inlet-outlet channel pairs fabricated in glass and isolated by the 10 × 10 array of holes visible in the gasket on the reactor face. Right. Schematic of the microreactor array operation. Gases flow into and out of the microreactor array through capillary tubes. The CSAF is sandwiched between a heater and the gasket. The holes in the gasket isolate 100 regions of the CSAF surface and one inlet–outlet pair.

formation of a Pd hydride phase with different electronic structure and reactivity than the alloy.

Surface Structure Spread Single Crystals

In the field of surface science a typical experiment is the study of a reaction on a single crystal surface. As a specific example, the surfaces of face-centered cubic metals have been studied extensively, and these crystals are often commercially available with any desired surface orientation, although the low Miller index orientations are by far the most common. A typical single crystal is approximately 1 cm in diameter and polished to a mirror finish with the surface crystallographic orientation known to $<0.5^{\circ}$ accuracy. When used in ultrahigh vacuum (UHV) surface science instruments, these surfaces can be cleaned and characterized by a variety of spectroscopic and microscopic methods to prepare well-defined surfaces that are often well-ordered atomically. Decades of work using this approach has developed substantial insights in catalysis, tribology, and other areas of surface related research. These types of studies have been used to explore the structure sensitivity of surface reactions by detailed studies of reactions on different surface orientations.[42]

The main drawbacks of single crystal surface science are the cost of the single crystals, and that the experiments can be very time consuming. Typically only one crystal orientation can be studied at a time, and it is laborious to open a UHV surface science chamber, change the crystal, and recondition the chamber afterwards to do experiments on a new crystal. Thus, progress in understanding structure sensitivity in chemical reactions on surfaces has been slow, but steady. Progress in surface science on materials that do not readily form large single crystals (e.g., some oxides) is practically non-existent.

A typical single crystal exposes a single surface orientation, ideally with an orientation that is known to high degree of accuracy, $<0.5^{\circ}$. This provides approximately 1 cm^2 of clean, well-defined surface area on which to perform experiments. An alternative approach is to use a single crystal with a similarly precise, but spherical surface[43]; a surface structure spread single crystal (S^4 C). On such a crystal the surface normal will vary across the crystal surface, exposing a broad continuous distribution of surface orientations. When coupled with characterization methods that have high spatial resolution, this

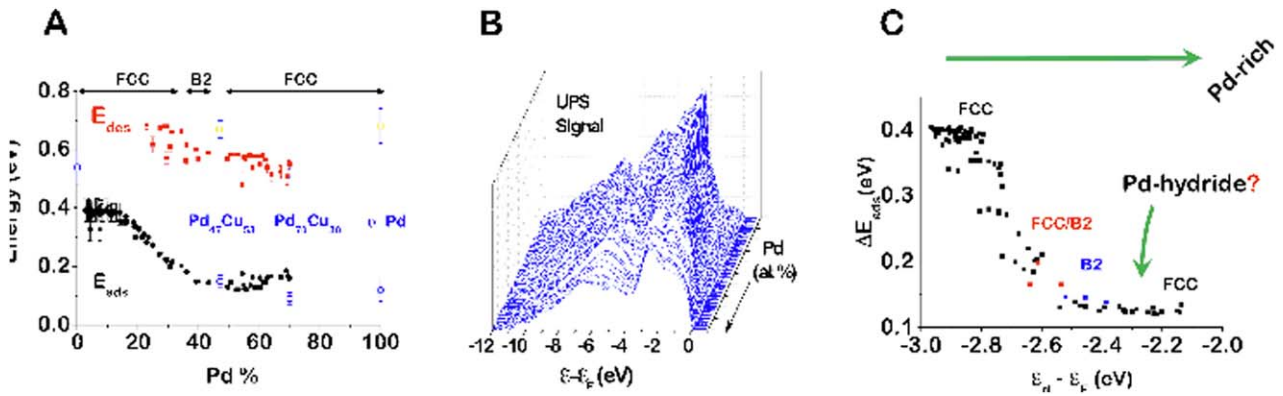

Figure 4. (A) Plot of the barriers to dissociative adsorption of H_2, and the recombinative desorption of H_2 on Cu_xPd_{1-x} alloys as determined from measurements of H_2-D_2 exchange kinetics on a Cu_xPd_{1-x} CSAF using the 100 channel microreactor array. The data in blue are estimates determined from H_2-D_2 exchange in a standard flow reactor and for catalysts of single composition. (B) UV photoemission spectra of Cu_xPd_{1-x} alloys. Increasing Pd content results in a shift of the valence band toward the Fermi level (0 eV). (C) Correlation of the barrier to H_2 adsorption with the average energy of the *d*-band electrons in Cu_xPd_{1-x} alloys.

enables many surface orientations to be studied on one sample and in one set of experiments. A single S^4 C sample cannot practically cover the entire range of crystallographic surfaces that are possible, but as few as six crystals with different primary orientations can span the entire stereographic triangle, enabling high-throughput studies of the structure sensitivity of surface reactions.

As a specific example, the initial stages of oxidation of Cu single crystal surfaces was studied using a Cu S^4 C of exposing all possible surface orientations lying within 10° of the (111) surface.[44] The (111) surface was approximately in the center of the crystal, and scanning tunneling microscopy showed that the step density on the surface increased with distance from the center in the expected way. The orientations of the step edges rotated as expected at various positions around the center. XPS was used to measure the oxygen uptake on the S^4 C surface at ~100 different surface orientations (Figure 5). By knowing the position of the XPS beam with respect to an origin on the crystal, the surface orientation at the beam position can be calculated, enabling a mapping of the XPS spectra vs. the surface orientation. The oxygen uptake depended only on the step density, and increased with distance from the (111) origin toward the edges of the crystal. Surprisingly, the step orientation and kink density had no apparent effect on the oxygen uptake.

Although they have been used sporadically over the many decades of modern surface science, the use of S^4 Cs is not common. Nonetheless, there are some other examples in the current literature. For example, water desorption on a curved Ag crystal was recently reported.[45] Those authors observed a significant linear dependence of the desorption temperature on the step density of the surface. It is likely this result could only have been observed on a curved crystal. This has important implications for benchmarking computational predictions of adsorption energies on surfaces of varying structure.

Nanoparticle Arrays

In the previous sections we described gradients in composition across alloy surfaces and surface orientation on single crystal surfaces. These are model surfaces that can often be characterized in atomic detail. Many catalysts, however, are based on nanoparticles. It is known that the catalytic activity of nanoparticles can depend on their size, with CO oxidation on Au serving as a classic example.[46] Given that the catalytic activity of nanoparticles may depend on the composition, size, and even the shape of the nanoparticles,[47] it is a significant challenge to map these properties using a traditional synthesis approach. It is very challenging to make a single particle size, or composition, and the resulting distribution makes it difficult to understand how it dictates the properties of interest.

A solution to this problem is to create surfaces with a gradient of particle size. For example, Hayden and coworkers prepared an array of Pt nanoparticles with a gradient in particle size across a TiO_2 thin film supported on a device they designed for high-throughput spatially resolved measurements.[48–50] The titania film was created by vapor deposition of Ti in the presence of oxygen. The Pt particles were created by atomic vapor deposition, and characterized by atomic force microscopy and ellipsometry. This enabled the formation of a single sample with a gradient in the thickness of Pt that ranged from 0.2 to 2 nm in equivalent thickness across the sample. During subsequent annealing, dewetting of the film from the substrate resulted in the formation of nanoparticles. The silicon substrate contained a 10 × 10 array of electrodes which could be individually addressed, enabling the properties of the nanoparticles to be probed with spatial resolution. They used this method to show that Pt exhibits particle size dependent oxidation stability, which has implications in electrochemical oxidation reactions. They found that it is more difficult to electrochemically oxidize CO, i.e., it is slower, on smaller Pt

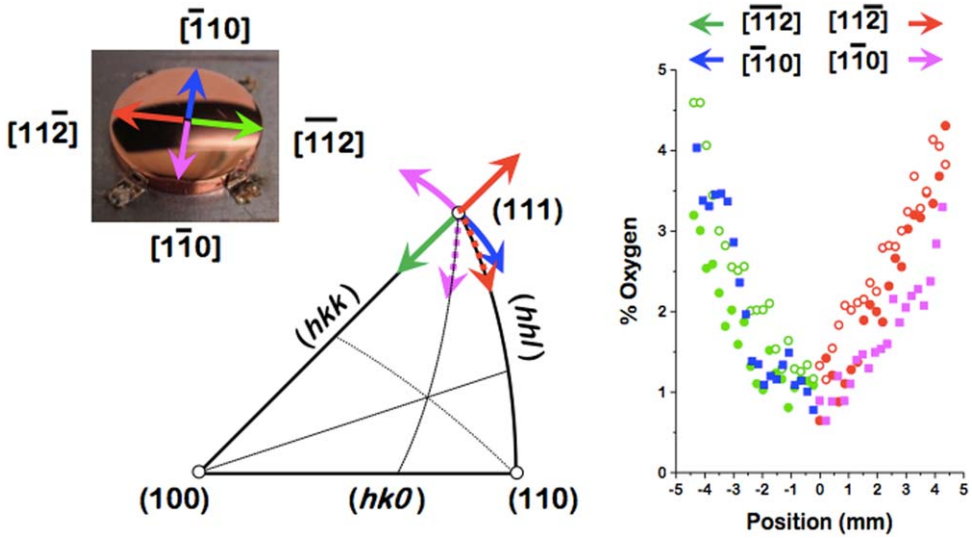

Figure 5. Left. Photograph of a a Cu(111) S^4C single crystals that is polished to a spherical dome shape. The arrows indicate the crystallographic directions also illustrated on the stereographic projection. The surface orientations along these directions expose monoatomic step edges separating (111) terraces. The step density increases with distance from the central (111) pole. Right. Uptake of oxygen on the surface during room temperature exposure to 30 L of O_2. The oxygen uptake increases as a function of distance from the (111) pole but does not depend on step orientation.

nanoparticles due to the difficulty of forming Pt-OH on the smaller particles. For the same reason, that makes it more difficult to reduce oxygen in the oxygen reduction reaction. Thus, the smallest Pt nanoparticles, while desirable for atom economy in a fuel cell, are simultaneously poisoned by CO and poor at oxygen reduction compared to larger nanoparticles.

Another application of nanoparticle size spreads examined the CO electro-oxidation activity of Au nanoparticles supported on titania films.[51] Gradients in particle size were created on a chip with a 10×10 array of electrodes. The particle sizes were characterized by transmission electron microscopy, and were 1–6 nm in diameter. Hayden et al. observed a maximum in CO oxidation activity at a particle diameter of about 3 nm. Interestingly, when the Au particles were supported on carbon films, they were not active at all.

An alternative approach to making gradients in nanostructures on a surface is the spinodal dewetting of a thin metal film on a silicon surface.[52] For example, a thin film of Pd evaporated onto a silicon single crystal substrate can be made to dewet by heating the surface. On dewetting, the Pd can sinter into balls and form a variety of structures depending on the film thickness and heating/annealing procedures. By depositing the initial films with a gradient in thickness and/or composition, it is possible to make gradients in nanostructure morphology and composition, which can then be studied using methods with high spatial resolution.

The ability to make controlled gradients in nanoparticle size and composition in samples where a property can be measured with high spatial resolution and attributed to local characteristics of the nanoparticles is a significant advance in nanoparticle science. This approach minimizes variations in reaction conditions between experiments, reduces the effects of particle size and composition distributions within a measurement, and provides a data-rich, nearly continuous trend in property-structure relationships.

Electrocatalysis

As alluded to in the previous section, high-throughput experimentation in electrocatalysis is comparatively common. This is in part because chips with individually addressable electrodes can be readily fabricated, allowing discrete sampling with high spatial resolution. This approach has been used to identify optimal materials for Li battery anodes,[53] electrochromic materials,[54] and fuel cell electrocatalysts.[55] Composition gradient films have been used in high throughput studies of ternary alloys for the oxygen reduction reaction,[56] and on CuPd alloys for nitrate electroreduction in water treatment.[57] Below we discuss two specific examples in electrocatalysis that highlight the use of composition gradient samples. This approach is notably different from high-throughput combinatorial experiments that use discrete samples (even at different compositions).[58–60]

The hydrogen evolution reaction (HER) and oxidation reaction (HOR) are two critical reactions in energy storage and conversion. HER is relevant for water splitting, and HOR is a potential fuel reaction in fuel cells. Alloys are often used in these reactions, and as described before, computational identification of optimal compositions is challenging due to effects of segregation. A study of the HOR/HER on PdAu alloys using a composition gradient film on addressable electrodes revealed interesting results.[61] First, there was a maximum in geometric activity near 70 at% Au for both reactions. This composition tends to have significant concentrations of Pd dimer and trimer ensembles. Second, HER persists at higher Au concentrations at lower activity. The HOR, in contrast, seems to shut off at $\approx$90 at% Au. Both reactions are poisoned by CO.

In a high-throughput computational study, Greeley et al. identified PtBi as a potential electrocatalyst for the HER.[12] In the previous example, the activity of Pd was promoted by alloying with a more inert metal. Consequently, an investigation of PdBi alloys was undertaken using a composition gradient sample with an array of electrodes as previously described.[62] Promotion effects were also observed, although they were not as strong as those observed in the PdAu work, and they were attributed to the formation of an αBi_2Pd intermetallic phase. Depending on the activity measure, the intermetallic phase is as active as pure Pd, but Bi is considerably cheaper than Pd, and the intermetallic phase does not form a hydride as pure Pd does, so it has some cost and stability advantages.

Outlook for High-Throughput Methods in Chemical Engineering

As illustrated, high throughput methods have enormous potential for impact in chemical engineering and across the engineering R&D domain, in general. The examples used above have focused on the problems with which we are most familiar, those related to processes at surfaces. Nonetheless, they provide some general sense of the methodology and the breadth of its potential reach across materials research.

The library containing a large number of samples is core to the physical implementation of many high throughput methods. The CSAF library that we use is one of many such libraries. CSAFs already have a long history, having first been developed in the 1950s as a platform for determining phase diagrams across continuous ranges of composition space.[63] There are a variety of methods for creating films with composition gradients, some as simple as dip-coating from solution and others requiring more sophisticated vacuum deposition tools. Another common implementation of a library is the use of robotic tools to prepare arrays of materials with discrete compositions at each point that need not be related to those of their neighbors, as is the case for CSAFs. The point is that the capital investment into equipment for library preparation can vary significantly, but need not be prohibitive.

The second common feature of high throughput methods is the use of a suite of methods for spatially resolved characterization of the materials in the library. These can include optical microscopy, electron microscopy, energy dispersive x-ray spectroscopy, Raman spectroscopy, photoemission, x-ray diffraction, etc. At a bare minimum it is necessary to determine local materials composition at points of interest across the physical extent of the library. To derive maximum value from a high throughput investigation, the degree and care with which materials characterization should be performed should be no less than would be done for any equivalent study using discrete composition samples. Without such characterization one cannot hope to model or understand the origins of trends in the functional properties that are the target of interest.

Simply knowing how a property depends on materials composition is a minimum bar.

The third leg of the experimental portion of a high throughput investigation is the measurement of the functional property of interest: catalysis, corrosion resistance, mechanical properties, electronic properties, fluorescence, membrane transport, etc. and the list could go on. Many of the materials characterization methods just mentioned are spatially resolved and simply need some degree of automation. High throughput measurements of some functional materials properties such as fluorescence need nothing more than a digital camera for data collection. However, many functional materials properties such as catalytic activity are not as readily measured in a parallelized mode. Development of methods for high throughput measurement of properties such as membrane transport, absorption, adhesion, and others is an area of significant opportunity for experimental research.

An obvious consequence of a working high throughput methodology is the generation of vastly greater quantities of data than can be analyzed by the individual researcher without the aid of trustworthy computational tools for modeling, data fitting, parameter estimation, and visualization. These are certainly areas of opportunity in research, but also for development of educational tools to teach practitioners how to extract the greatest value from the data gusher. While the quality of data and the amount available will greatly exceed past norms, their value will not be realized without rigorous analysis. In the same vein, there is a need to understand appropriate design of experiments methods to ensure that the data collected spans the requisite parameter space. In applications of high throughput methods that are simply aimed at identifying "optimal" materials, there is a need for screening protocols that will sample multidimensional materials descriptor spaces as efficiently as possible. The same efficiency of sampling is just as necessary in studies aimed at developing models or verifying hypotheses regarding the composition dependence of a given materials property.

Finally, there is the role of computational materials simulation, which must be used in partnership with experiment to interpret the observations of high throughput studies at the atomistic level. Simulation is challenged equally, if not more so, by multicomponent materials. Simulation must handle the same continuous multidimensional composition spaces and, at every composition, the multitude of atomic configurations accessible. Methods that extend the reach of first-principles simulations, such as cluster expansions and accurate force fields will be needed to accomplish this with the accuracy expected of electronic structure methods. New multiscale simulation methods will be needed to examine materials properties that depend on meso and microstructure properties, or which change over time.

Both experimental and computational high-throughput methods face the challenge of how to archive the scientific products that result from their use. Standard publications can report distilled observations and conclusions, but they struggle to adequately archive very large datasets. New approaches to archiving data sets will have to be developed, e.g., using data repositories. For example, we archived a medium sized ($\sim$1.8 GB) dataset of DFT calculations[64] in Zenodo[65] in one publication. Other repositories exist as well, including institutional repositories, Figshare,[66] as well as domain specific solutions including the Materials Project.[2] These solutions continue to evolve to solve data archiving and reusability challenges.

Over the next decade, high throughput methods will enable the study and solution of scientific and engineering problems relevant to Chemical Engineering and, in the context of this perspective, problems related to multicomponent materials. These methods have been adopted whole-heartedly by many corporate R&D labs in the business of product development, to accelerate the screening of product materials and accelerate the optimization processes for their production. In many cases, the investments have been large enough that only the R&D arms of major corporations can afford to make them. However, for enterprises with smaller research budgets and for academics these tools need not be prohibitively expensive. Furthermore, there are still roles to be played by academia in the development of new experimental methods, tools for data reduction and methods for computational simulation to augment high throughput experimentation.

Acknowledgments

AJG acknowledges support for work described in this perspective performed under NSF grant CBET-0923083 and DOE grant DE-FE0004000. JRK gratefully acknowledges the partial support from the DOE Office of Science Early Career Research program (DE-SC0004031).

Literature Cited

1. Materials genome initiative. https://www.mgi.gov.
2. Jain A, Ong SP, Hautier G, Chen W, Richards WD, Dacek S, Cholia S, Gunter D, Skinner D, Ceder G, Persson KA. The materials project: a materials genome approach to accelerating materials innovation. *APL Materials* 2013;1(1):011002.
3. Hattrick-Simpers J, Wen C, Lauterbach J. The materials super highway: integrating high-throughput experimentation into mapping the catalysis materials genome. *Catal Lett*. 2014;145(1):290–298.
4. Studt F, Abild-Pedersen F, Bligaard T, Sørensen RZ, Christensen CH, Nørskov JK. Identification of non-precious metal alloy catalysts for selective hydrogenation of acetylene. *Science* 2008;320(5881):1320–1322.
5. Potyrailo R, Rajan K, Stoewe K, Takeuchi I, Chisholm B, Lam H. Combinatorial and high-throughput screening of materials libraries: review of state of the art. *ACS Combinat Sci*. 2011;13(6):579–633.
6. Farrusseng D. High-throughput heterogeneous catalysis. *Surf Sci Rep*. 2008;63(11):487–513.
7. Turner HW, Volpe AF, Weinberg WH. High-throughput heterogeneous catalyst research. *Surf Sci*. 2009;603(10–12):1763–1769.
8. Devore DD, Jenkins RM. Impact of high throughput experimentation on homogeneous catalysis research. *Comm Inorgan Chem*. 2014;34(1–2):17–41.
9. Sundermann A, Gerlach O. High-throughput screening technology for automotive applications. *Chemie Ingenieur Technik*. 2014;86(11):1941–1947.

10. Curtarolo S, Morgan D, Persson K, Rodgers J, Ceder G. Predicting crystal structures with data mining of quantum calculations. *Phys Rev Lett*. 2003;91(13):135503.
11. Morgan D, Ceder G, Curtarolo S. High-throughput and data mining with ab initio methods. *Measure Sci Technol*. 2005;16(1):296–301.
12. Greeley J, Jaramillo TF, Bonde J, Chorkendorff I, Nørskov JK. Computational high-throughput screening of electrocatalytic materials for hydrogen evolution. *Nat Mater*. 2006;5(11):909–913.
13. Setyawan W, Curtarolo S. High-throughput electronic band structure calculations: challenges and tools. *Comput Mater Sci*. 2010;49(2):299–312.
14. Jain A, Hautier G, Moore CJ, Ong SP, Fischer CC, Mueller T, Persson KA, Ceder G. A high-throughput infrastructure for density functional theory calculations. *Comput Mater Sci*. 2011;50(8):2295–2310.
15. Curtarolo S, Setyawan W, Hart GLW, Jahnatek M, Chepulskii RV, Taylor RH, Wang S, Xue J, Yang K, Levy O, Mehl MJ, Stokes HT, Demchenko DO, Morgan D. Aflow: an automatic framework for high-throughput materials discovery. *Comput Mater Sci*. 2012;58(0):218–226.
16. Curtarolo S, Hart GLW, Nardelli MB, Mingo N, Sanvito S, Levy O. The high-throughput highway to computational materials design. *Nat Mater*. 2013;12(3):191–201.
17. Toher C, Plata JJ, Levy O, de Jong M, Asta M, Nardelli MB, Curtarolo S. High-throughput computational screening of thermal conductivity, debye temperature, and grüneisen parameter using a quasiharmonic debye model. *Phys Rev B*. 2014;90(17):174107.
18. Guerin S, Hayden BE. Physical vapor deposition method for the high-throughput synthesis of solid-state material libraries. *J Comb Chem*. 2006;8(1):66–73.
19. Takeuchi I, van Dover RB, Koinuma H. Combinatorial synthesis and evaluation of functional inorganic materials using thin-film techniques. *MRS Bull*. 2002;27(04):301–308.
20. van Dover RB, Schneemeyer LF. The codeposited composition spread approach to high-throughput discovery/exploration of inorganic materials. *Macromol Rapid Commun*. 2004;25(1):150–157.
21. Ludwig A, Zarnetta R, Hamann S, Savan A, Thienhaus S. Development of multifunctional thin films using high-throughput experimentation methods. *Int J Mater Res*. 2008;99(10):1144–1149.
22. Priyadarshini D, Kondratyuk P, Miller JB, Gellman AJ. Compact tool for deposition of composition spread alloy films. *J Vacuum Sci Technol A*. 2012;30(1):011503–1–011503–8.
23. Fleutot B, Miller JB, Gellman AJ. Apparatus for deposition of composition spread alloy films: the rotatable shadow mask. *J Vacuum Sci Technol A*. 2012;30(6):061511.
24. Aljohani TA, Hayden BE, Anastasopoulos A. The high throughput electrochemical screening of the corrosion resistance of Ni-Cr thin film alloys. *Electrochimica Acta*. 2012;76:389–393.
25. Bunn JK, Fang RL, Albing MR, Mehta A, Kramer MJ, Besser MF, Hattrick-Simpers JR. A high-throughput investigation of fe-cr-al as a novel high-temperature coating for nuclear cladding materials. *Nanotechnology*. 2015;26(27):274003.
26. Payne MA, Miller JB, Gellman AJ. High-throughput characterization of early oxidation across Al_x Fe_y Ni_{1-x-y} composition space. *Corros Sci*. 2015;91:46–57.
27. König D, Eberling C, Kieschnick M, Virtanen S, Ludwig A. High-throughput investigation of the oxidation and phase constitution of thin-film ni-al-cr materials libraries. *Adv Eng Mater*. 2015;17(9):1365–1373.
28. Wagner C. Reaktionstypen bei der oxydation von legierungen. *Zeitschrift Fur Elektrochemie*. 1959;63:772–790.
29. Sinfelt JH. Catalysis by alloys and bimetallic clusters. *Account Chem Res*. 1977;10(1):15–20.
30. Priyadarshini D, Kondratyuk P, Picard YN, Morreale BD, Gellman AJ, Miller JB. High-throughput characterization of surface segregation in Cu_xPd_{1-x} alloys. *J Phys Chem C*. 2011;115(20):10155–10163.
31. Subramanian PR, Laughlin DE. Cu-Pd (copper-palladium). *J Phase Equil*. 1991;12(2):231–243.
32. Boes J, Kondratyuk P, Yin C, Miller JB, Gellman AJ, Kitchin JR. Core level shifts in Cu-Pd alloys as a function of bulk composition and structure. *Surf Sci*. 2015;640:127–132.
33. Mårtensson N, Nyholm R, Calén H, Hedman J, Johansson B. Electron-spectroscopic studies of the Cu_xPd_{1-x} alloy system: chemical-shift effects and valence-electron spectra. *Phys Rev B*. 1981;24(4):1725–1738.
34. Cole RJ, Brooks NJ, Weightman P. Determination of charge transfer in the Cu_xPd_{1-x} alloy system. *Phys Rev B*. 1997;56:12178–12182.
35. Senkan S, Krantz K, Ozturk S, Zengin V, Onal I. High-throughput testing of heterogeneous catalyst libraries using array microreactors and mass spectrometry. *Angewandte Chemie International Edition*. 1999;38(18):2794–2799.
36. Snively CM, Oskarsdottir G, Lauterbach J. Parallel analysis of the reaction products from combinatorial catalyst libraries. *Angewandte Chemie International Edition*. 2001;40(16):3028–3030.
37. Snively CM, Oskarsdottir G, Lauterbach J. Chemically sensitive parallel analysis of combinatorial catalyst libraries. *Catal Today*. 2001;67(4):357–368.
38. Senkan SM. High-throughput screening of solid-state catalyst libraries. *Nature*. 1998;394(6691):350–353.
39. Kondratyuk P, Gumuslu G, Shukla S, Miller JB, Morreale BD, Gellman AJ. A microreactor array for spatially resolved measurement of catalytic activity for high-throughput catalysis science. *J Catal*. 2013;300:55–62.
40. Gumuslu G, Kondratyuk P, Boes JR, Morreale B, Miller JB, Kitchin JR, Gellman AJ. Correlation of electronic structure with catalytic activity: H_2-D_2 exchange across Cu_xPd_{1-x} composition space. *ACS Catal*. 2015;5(5):3137–3147.
41. Boes JR, Gumuslu G, Miller JB, Gellman AJ, Kitchin JR. Estimating bulk-composition-dependent H_2 adsorption energies on Cu_xPd_{1-x} alloy (111) surfaces. *ACS Catal*. 2015;5:1020–1026.

42. Somorjai GA, Carrazza J. Structure sensitivity of catalytic reactions. *Ind Eng Chem Fund.* 1986;25(1):63–69.
43. de Alwis A, Holsclaw B, Pushkarev VV, Reinicker A, Lawton TJ, Blecher ME, Sykes ECH, Gellman AJ. Surface structure spread single crystals (S4C): preparation and characterization. *Surf Sci.* 2013;608:80–87.
44. Lawton TJ, Pushkarev V, Broitman E, Reinicker A, Sykes ECH, Gellman AJ. Initial oxidation of Cu(hkl) surfaces vicinal to Cu(111): a high-throughput study of structure sensitivity. *J Phys Chem C.* 2012;116(30): 16054–16062.
45. Janlamool J, Bashlakov D, Berg O, Praserthdam P, Jongsomjit B, Juurlink L. Desorption of water from distinct step types on a curved silver crystal. *Molecules.* 2014;19(8):10845–10862.
46. Valden M. Onset of catalytic activity of gold clusters on titania with the appearance of nonmetallic properties. *Science* 1998;281(5383):1647–1650.
47. Kim S, Lee D.W, Lee KY. Shape-dependent catalytic activity of palladium nanoparticles for the direct synthesis of hydrogen peroxide from hydrogen and oxygen. *J Mol Catal A.* 2014;391:48–54.
48. Hayden BE, Pletcher D, Suchsland JP, Williams LJ. The influence of pt particle size on the surface oxidation of titania supported platinum. *Phys Chem Chem Phys.* 2009;11(10):1564.
49. Hayden BE, Pletcher D, Suchsland JP, Williams LJ. The influence of support and particle size on the platinum catalysed oxygen reduction reaction. *Phys Chem Chem Phys.* 2009;11(40):9141.
50. Brian E. Hayden. Particle size and support effects in electrocatalysis. *Accounts of Chemical Research*, 46(8): 1858–1866, 2013.
51. Hayden BE, Pletcher D, Suchsland JP. Enhanced activity for electrocatalytic oxidation of carbon monoxide on titania-supported gold nanoparticles. *Angew Chem Int Ed.* 2007;46(19):3530–3532.
52. Michalak WD, Miller JB, Yolcu C, Gellman AJ. Fabrication of metallic nanoparticles by spinodal dewetting of thin films: a high-throughput approach. *Thin Solid Films* 2012;522:473–479.
53. Spong AD, Vitins G, Guerin S, Hayden BE, Russell AE, Owen JR. Combinatorial arrays and parallel screening for positive electrode discovery. *J Power Sources* 2003; 119–121:778–783.
54. Brace KM, Hayden BE, Russell AE, Owen JR. A parallel optical screen for the rapid combinatorial electrochromic analysis of electrochemical materials. *Adv Mater.* 2006;18(24):3253–3257.
55. Guerin S, Hayden BE, Lee CE, Mormiche C, Owen JR, Russell AE, Theobald B, Thompsett D. Combinatorial electrochemical screening of fuel cell electrocatalysts. *J Comb Chem.* 2004;6(1):149–158.
56. Guerin S, Hayden BE, Lee CE, Mormiche C, Russell AE. High-throughput synthesis and screening of ternary metal alloys for electrocatalysis. *J Phys Chem B.* 2006; 110(29):14355–14362.
57. Anastasopoulos A, Hannah L, Hayden BE. High throughput optimisation of PdCu alloy electrocatalysts for the reduction of nitrate ions. *J Catal.* 2013;305:27–35.
58. Gurau B, Viswanathan R, Liu RX, Lafrenz TJ, Ley KL, Smotkin ES, Reddington E, Sapienza A, Chan BC, Mallouk TE, Sarangapani S. Structural and electrochemical characterization of binary, ternary, and quaternary platinum alloy catalysts for methanol electro-oxidation. *J Phys Chem B.* 1998;102(49):9997–10003.
59. Reddington E, Sapienza A, Gurau B, Viswanathan R, Sarangapani A, Smotkin ES, Mallouk TE. Combinatorial electrochemistry: a highly parallel, optical screening method for discovery of better electrocatalysts. *Science.* 1998;280(5370):1735–1737.
60. Liu R, Smotkin ES. Array membrane electrode assemblies for high throughput screening of direct methanol fuel cell anode catalysts. *J Electroanal Chem.* 2002;535(1–2): 49–55.
61. Al-Odail FA, Anastasopoulos A, Hayden BE. The hydrogen evolution reaction and hydrogen oxidation reaction on thin film PdAu alloy surfaces. *Phys Chem Chem Phys.* 2010;12(37):11398.
62. Al-Odail FA, Anastasopoulos A, Hayden BE. Hydrogen evolution and hydrogen oxidation on palladium bismuth alloys. *Topic Catal.* 2011;54(1–4):77–82.
63. Boettcher A, Haase G, Thun R. Strukturuntersuchung von mehrstoffsystemen durch kinematische elektronenbeugung. *Z Metallkd.* 1955;46:386–400.
64. Xu Z, Rossmeisl J, Kitchin JR. Supporting data for: a linear response, DFT+U study of trends in the oxygen evolution activity of transition metal rutile dioxides. doi:10.5281/zenodo.12635, 2015.
65. Zenodo. https://zenodo.org. Zenodo builds and operate a simple and innovative service that enables researchers, scientists, EU projects and institutions to share and showcase multidisciplinary research results (data and publications) that are not part of the existing institutional or subject-based repositories of the research communities.
66. figshare. http://figshare.com. figshare helps academic institutions store, share and manage all of their research outputs. Accessed May 16, 2016.